Dynamics of DNA Condensates at the Solid−Liquid Interface by Atomic Force Microscopy

Michele Y. Ono and Eileen M. Spain*

Contribution from the Department of Chemistry, Occidental College, 1600 Campus Road, Los Angeles, California 90041

Received May 11, 1999

Abstract: Real-time dynamics of the interaction of two DNA condensates are imaged with atomic force microscopy under fluid. DNA condensates are formed at the solid−liquid interface of aqueous buffer and chemically modified mica. Atomic force microscopy shows that the DNA condensates and the strands that compose these condensates interact and are dynamic in fluid. For the first time, images of two closely spaced condensates show that the strands in one condensate organize commensurately with the nearby strands of the second condensate. The observed structure may be an intermediate for a multi-condensate toroid. The implications of this finding are considered.

Introduction

There is great interest in elucidating the mechanisms of deoxyribonucleic acid (DNA) condensation.[1] Packing of DNA into a condensed form is required for several cellular processes. One of these is mitosis in eukaryotic cells. Histones and other proteins are employed to compact the DNA into chromatin. In turn, chromatin becomes organized into chromosomes during the metaphase of mitosis.[2] DNA condensation is also relevant in gene transfer.[1−4] In these kinds of cellular processes, the change in volume of DNA packed to unpacked may vary over several orders of magnitude.[1,2] For example, DNA compaction into chromosomes is necessary because the length of DNA may vary up to 100 000 times the length of the cell.[2] There is much to be learned about the mechanism of these remarkable packing and unraveling processes.

In the early 1990s, Bloomfield *et al*.[5] discovered that it is possible to mimic DNA compaction *in vitro* using multivalent cations. When adsorbed onto a surface, these compacted structures are termed DNA condensates and have been imaged by electron microscopy (EM).[5] Therefore, this *in vitro* system can serve as a model for DNA compaction *in vivo*. Cryogenic electron microscopy by Bottcher *et al*.[6] provides images of intermediates in spermine/uranyl salt-induced condensates of linearized DNA. Spermine and a similar species, spermidine, are polyamines thought to be used in prokaryotes to counteract the negative charge of DNA's phosphate groups and facilitate compaction.[2]

Very recently DNA condensates have been observed using atomic force microscopy (AFM).[3,4,7−10] These studies employed chemically modified or cationic-treated surfaces. Agents such as polyamines,[3,8,10] glycoproteins,[4] protamines,[7] and cationic moieties at or near the mica surface[9] were used to induce DNA condensation. Various condensate structures such as rods, flowers, and toroids were observed. These electron and atomic force microscopy studies all suggested the following: that parallel chains form linear structures, and that once these linear structures are formed, they aggregate to form multimeric condensates.

An advantage of AFM over EM is the possibility of observing dynamics in fluid. With the exception of the study by Dunlap *et al*.,[3] all of the aforementioned AFM studies took place in air. At best, such studies provided snapshots of reactants, intermediates, and products that depended upon reaction time or conditions. However, potential artifactual effects due to drying of the aqueous deposition solution prior to AFM observation cannot be ignored entirely.[4,8,9,11] We are aware of only a few AFM studies of biologically interesting systems that are imaged under fluid. These studies include DNA−enzyme reactions *in situ* by Guthold *et al*.[12] and Bezanilla *et al*.,[13] an enzyme−substrate interaction by Radmacher *et al*.,[14] replication,[15] transcription,[16] and the motion of supercoiled DNA on chemically modified mica.[17]

* To whom correspondence should be addressed. E-mail: emspain@oxy.edu.

(1) Bloomfield, V. A. *Curr. Opin. Struct. Biol*. **1996**, *6*, 334−341 and references therein.

(2) Lodish, H.; Baltimore, D.; Berk, A.; Zipursky, S. L.; Matsidaira, P.; Darnell, J. *Molecular Cell Biology*; W. H. Freeman and Company: New York, 1997.

(3) Dunlap, D. D.; Maggi, A.; Soria, M. R.; Monaco, L. *Nucleic Acids Res.* **1997**, *25*, 3095−3101.

(4) Hansma, H. G.; Golan, R.; Hsieh, W.; Lollo, C. P.; Mullen-Ley, P.; Kwoh, D. *Nucleic Acids Res.* **1998**, *26*, 2481−2487.

(5) Ma, C.; Bloomfield, V. A. *Biophys. J*. **1994**, *67*, 1678−1681 and references therein.

(6) Bottcher, C.; Endisch, C.; Fuhrhop, J.-H.; Catterall, C.; Eaton, M. *J. Am. Chem. Soc*. **1998**, *120*, 12−17.

(7) Allen, M. J.; Bradbury, E. M.; Balhorn, R. *Nucleic Acids Res.* **1997**, *25*, 2221−2226 and references therein.

(8) Fang, Y.; Hoh, J. H. *J. Am. Chem. Soc*. **1998**, *120*, 8903−8909.

(9) Fang, Y.; Hoh, J. H. *Nucleic Acids Res.* **1998**, *26*, 588−593. Fang, Y.; Spisz, T. S.; Hoh, J. H. *Nucleic Acids Res*. **1999**, *27*, 1943−1949.

(10) Lin, Z.; Wang, C.; Feng, X.; Liu, M.; Li, J.; Bai, C. *Nucleic Acids Res.* **1998**, *26*, 3228−3234.

(11) Wang, W.; Lin, J.; Schwartz, D. C. *Biophys. J.* **1998**, *75*, 513−520.

(12) Guthold, M.; Bezanilla, J.; Erie, D. A.; Jenkins, B.; Hansma, H. G.; Bustamante, C. *Proc. Natl. Acad. Sci. U.S.A.* **1994**, *91*, 12927−12931.

(13) Bezanilla, M.; Drake, B.; Nudler, E.; Kashlev, M.; Hansma, P. K.; Hansma, H. G. *Biophys. J.* **1994**, *67*, 2454−2459.

(14) Radmacher, M.; Fritz, M.; Hansma, H. G.; Hansma, P. K. *Science* **1994**, *265*, 1577−1579.

(15) Argaman, M.; Golan, R.; Thomson, H. H.; Hansma, H. G. *Nucleic Acids Res.* **1997**, *25*, 4379−4384.

10.1021/ja9915697 CCC: $18.00
Published on Web 07/30/1999

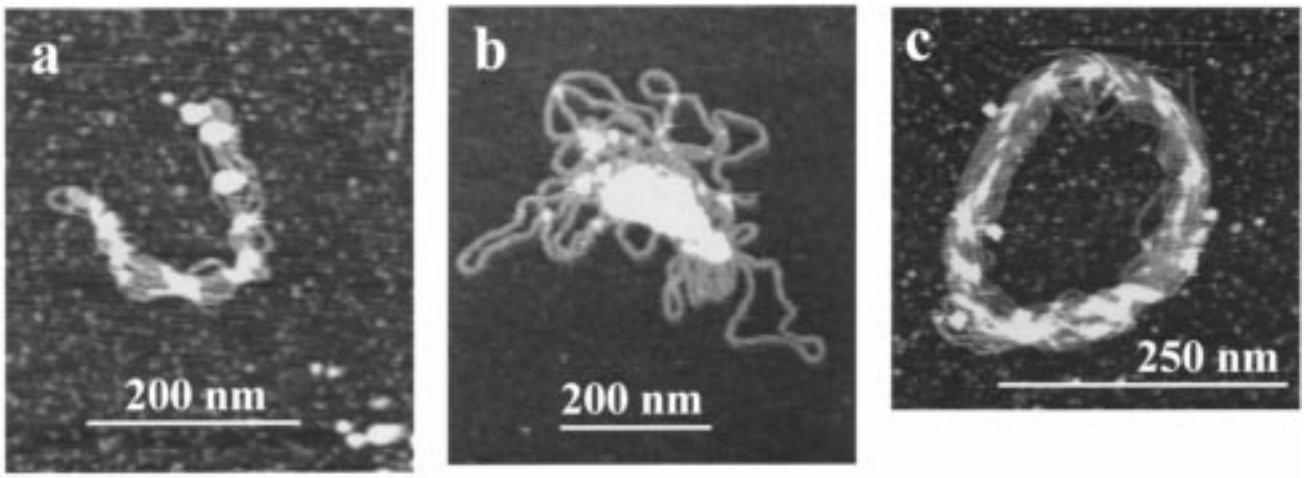

Figure 1. AFM images of condensate structures typically observed: (a) linear or rod composed of one plasmid, (b) flower, and (c) toroid that appears to be formed from two or more linear structures.

Another technique that is employed to study the kinetics and dynamics of DNA condensation is fluorescence microscopy. In aqueous solution, this technique was used to image the uncondensed (random coil) to condensed (globule) transition as a function of multivalent cation concentration.[18] Under these conditions, the condensation was found to be reversible. All in all, the dynamics studies are arguably the most important because they occur in real time and in an essentially natural environment. The fluorescence studies are advantageous in that no surface is required for aggregation; however, they lack the spatial resolution of AFM. The model system therefore should utilize AFM because it allows the visualization of dynamic processes under native conditions with high, spatial resolution.

There are recent theoretical investigations of DNA condensation in the literature. Liu and co-workers[19] undertook a study of the nonpairwise additive interactions among *n*-sized bundles of polyelectrolytic rods. In other theoretical studies based on a two-rod model,[20−23] short-range attractions between rods with condensed counterions account for condensate formation. Liu and co-workers set out to apply a new model to an *n*-sized bundle.[19] They found that an infinite number of rods bundle into a condensate due to counterion correlation across the bundle. Since these theoretical results contradict experimental findings, they proposed that nonelectrostatic forces may be responsible for finite-sized bundles. One such nonelectrostatic force that may be important has been determined in another theoretical study. Park and co-workers[24] were interested in understanding the size invariance of toroidal condensates formed in solution from a wide range of DNA lengths (400−50000 base pairs). Using a flexible rod model, they found the size invariance was due to crossover points (i.e. regions of nonparallel strands that are necessary to compact the DNA). Park *et al.* proposed that these topological defects and their energies are what determine toroid size. To our knowledge, no theoretical work on condensates at the solid−liquid interface has been performed.

Our interest lies in using the dynamics of condensate formation at the solid−liquid interface as a model for understanding the process *in vivo*. This model system closely resembles the cellular process in two ways; the experiment occurs in water and on a surface. In our experimental design, we observe the dynamics of inter-condensate formation with high-resolution AFM images obtained under fluid. We present the striking result that the strands of a transient state of an intercondensate structure can self-assemble.

Experimental Method

Sample and Substrate Preparation. A plasmid DNA pBR322 (Life Technologies, Grand Island, NY) of 4363 basepairs that is approximately 90% supercoiled was used as received. The pBR322 was diluted to 0.0004 μg/μL with sterile 10 mM Tris HCl, pH 7.6, 1 mM EDTA buffer. Ruby and green muscovite mica (Asheville-Schoonmaker Mica Company, Newport News, VA) with dimensions of 1/2 in. × 1/2 in. were used as substrates. A flat mica surface was obtained by cleavage with adhesive tape. With one exception, the cleaved ruby or green mica was submerged for 2 min in a solution of 1 % by volume 3-aminopropyltriethoxysilane (APTES) (99% purity, Acros, Pittsburgh, PA) in HPLC grade methanol (Fisher Scientific, Pittsburgh, PA).[25] The mica sample was rinsed with approximately 20 mL of HPLC grade methanol and kept in a covered Petri dish and allowed to dry.

Image Collection. All images were collected at room temperature under fluid using an AFM in the tapping mode (Digital Instruments, Nanoscope IIIa). The chemically modified or bare mica substrate was attached to a stainless steel disk and mounted on the microscope. An oxide-sharpened silicon nitride tip (Digital Instruments Inc., Santa Barbara, CA) or an oxide-sharpened oriented twin tip, each attached to a 100 μm cantilever with a force constant of 0.32 N/m, was lowered to the mica sample. Difficulties with attaining high-resolution images precluded us from using a sealed fluid cell. Instead, we simply imaged under a large water bead. As a result, time duration for imaging was reduced because the aqueous solution on the mica eventually evaporated. The total imaging time varied from 60 to 90 min.

Once the microscope was ready for imaging, the dried, chemically modified, or bare mica substrate was mounted. A 25 μL aliquot of the 0.0004 μg/μL aqueous solution of pBR322 (10 ng) was deposited onto the mica surface. For Figure 1b only, pBR322 was diluted in the buffer noted above plus 10 mM $NiCl_2$ and deposited onto bare mica. After

(16) Kasas, S.; Thomson, N. H.; Smith, B. L.; Hansma, H. G.; Zhu, X.; Guthold, M.; Bustamante, C.; Kool, E. T.; Kashlev, M.; Hansma, P. K. *Biochemistry* **1997**, *36*, 461−468.
(17) Lyubchenko, Y. L.; Shlyakhtenko, L. S. *Proc. Natl. Acad. Sci. U.S.A.* **1997**, *94*, 496−501.
(18) Takahashi, M.; Yoshikawa, K.; Vasilevskaya, V. V.; Khokhlov, A. R. *J. Phys. Chem. B* **1997**, *101*, 9396−9401. Melnikov, S. M.; Sergeyev, V. G.; Yoshikawa K. *J. Am. Chem. Soc.* **1995**, *117*, 9951−9956.
(19) Ha, B.-Y.; Liu, A. J. *Phys. Rev. Lett.* **1998**, *81*, 1011−1014.
(20) Gronbech-Jensen, N.; Mashl, R. J.; Bruinsma, R. F.; Gelbart, W. M. *Phys. Rev. Lett.* **1997**, *78*, 2477−2480.
(21) Ray, J.; Manning, G. S. *Langmuir* **1994**, *10*, 2450−2461.
(22) Barrat, J. L.; Joanny, J. F. *Adv. Chem. Phys.* **1996**, *94*, 1−66.
(23) Ha, B.-Y.; Liu, A. J. *Phys. Rev. Lett.* **1997**, *79*, 1289−1292.
(24) Park, S. Y.; Harries, D.; Gelbart, W. M. *Biophys. J.* **1998**, *75*, 714−720.
(25) Hu, J.; Wang, M.; Weier, H.-U.; Frantz, P.; Kolbe, W.; Ogletree, D. F.; Salmeron, M. *Langmuir* **1996**, *12*, 1697−1700.

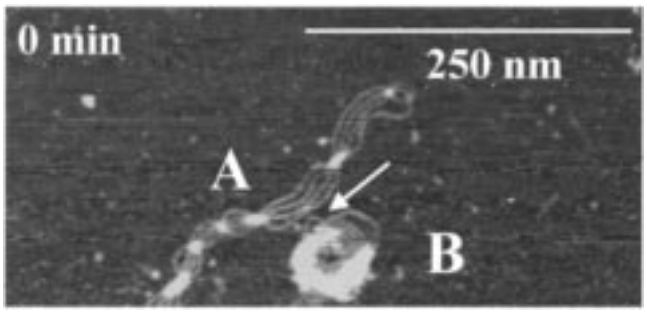

Figure 2. AFM image of two closely spaced condensates. Condensate **A** is a linear structure composed of one plasmid. Condensate **B** is a toroidal structure. The arrow indicates the position where a small loop of **B** is close to the crossover point of the two rightmost strands of **A**.

the oscillating cantilever was manually tuned, the DNA-mica surface was immediately imaged under aqueous solution. The time delay between DNA deposition and imaging varied from 1 to 3 min. Once the appropriate magnification to observe high-resolution images was achieved, approximately 5 min had elapsed since initial DNA deposition. Images were typically collected at scan rates of 1.5 to 2 Hz in height mode (constant cantilever oscillation amplitude). Figures 1a, 1c, 2, 3, and 4 were subjected to just one modification; the vertical offset between scan lines was removed. For a given image, this was accomplished by subtraction of the average vertical value of the scan line from each point in the scan line. Instrument software provided this modification procedure. No other modifications to the images were performed. No modification was applied to Figures 1b and 5. The height contrast was adjusted to 10 nm for all images.

Results

Figure 1 displays three representative AFM images of the condensate structures that we typically observe in aqueous solution: rod[9] or linear (Figure 1a); flower[4] (Figure 1b); and toroid (Figure 1c). These images, displayed in order of decreasing relative frequency of occurrence, are observed at the earliest times following DNA deposition. (Although Figure 1b was obtained with Ni^{2+}-treated mica, we observe the flower structure on APTES-modified mica with approximately the same relative frequency.) The length of the linear structure in Figure 1a is measured to be approximately 350 nm, and is most likely composed of one DNA plasmid. It contains several crossover points that are image areas of high contrast where DNA strands overlap or bundle tightly. These crossover points may contain cationic species as well. Somewhat less frequently, we observe two plasmids in a linear condensate. The flower structure imaged in Figure 1b is composed of one or two plasmids. The relatively few toroids observed under these experimental conditions are typically multimeric, as is the one shown in Figure 1c.

Figure 2 shows two DNA condensates (labeled **A** and **B**) that are in close proximity to one another. Condensate **A** is a linear structure composed of one plasmid, similar to that of Figure 1a, whereas condensate **B** is a toroid and is probably monomeric. The arrow in the figure indicates the focal point of subsequent dynamics. At the arrow, there are 4 strands of **A** and a strand of **B** directed toward a crossover point of **A**. The crossover point of **A** is composed of the two rightmost strands (out of 4 strands) of **A**. The 4 strands of **A** are packed closely and molded toward the crossover point of **A**. Condensate **A** is largely a 2-dimensional structure with the strands spread evenly on the surface, whereas **B** appears 3-dimensional.

From this starting point, we proceeded to collect as many images of this pair *in situ* as the instrument or our experimental setup allowed. Figure 3 shows a series of images collected over a time span of 23 min, (i.e., 25 min elapsed from Figure 2 to Figure 3i). The image of Figure 3a was collected 2 min following that of Figure 2, and no significant change has occurred. In Figure 3b, a noticeable change occurs; a loop representing part of a strand of **B** has dissociated from the toroid and has arranged itself commensurately with the strands of **A**. In addition, the inter-strand distance of the 4 strands of **A** has increased as compared with Figure 3a. After 5 min, the image in Figure 3c shows the loop from **B** moving into the space between **A** and **B**. In addition, the end of this strand is molding itself toward the curvature of the toroid. At the same time, the crossover point of **A** appears to have moved in that same direction. Now, condensate **B** is more 2-dimensional. After 6 min (Figure 3d), the two strands of the **B** loop are curved and parallel to the strands of **A** and **B**. Note here that once again, the 4 strands of **A** have compacted.

Yet another significant change occurs at 8 min (Figure 3e). The strands of the toroid are approximately parallel, evenly spaced, and organized. In addition, another part of the **B** strand moves toward **A**. There is now a crossover point of this new piece of the **B** loop (arrow in Figure 3e) that is arranged close to the crossover point of **A** (panels f and g in Figure 3). In panels f and g of Figure 3, the 4 strands of **A** adjust positions to the new crossover point of the **B** loop. Once again, by the end of the time series, the strands of **B** and the 4 strands of **A** are parallel and nearly equidistant. In addition, the strands of the **B** toroid are organized and the crossover points of **B** and **A** are in close proximity. The final two images collected in this series at 23 and 25 min, respectively, are shown in panels h and i of Figure 3. In these images, further formation of parallel strands on the surface is observed.

The dynamical event is summarized in Figure 4. Panels a and b in Figure 4 are the images at time zero and time 23 min, respectively. Over these 23 min, the toroid has lengthened along its resulting long axis by 10 ± 0.5 nm. Note that the long axis of the toroid is approximately parallel with the long axis of the linear structure. The toroid has become increasingly 2-dimensional, with the strands arranged on the surface in an organized manner. In addition, the 4 proximal strands of **A** have increased their separation and collinearity. We see in Figure 4c a magnification of Figure 4b. The inter-strand distance near the crossover point varies from 6.0 ± 0.1 to 7.0 ± 0.1 nm. Finally, we have observed many multi-condensate structures at early times following deposition. A representative image of such a structure is displayed in Figure 5. Here we notice that three or four linear structures have formed a roughly circular, multi-condensate structure.

Discussion

In this work, we have observed the dynamics of inter-condensate structure formation *in situ*. For the time series data, DNA deposition takes place in solution on APTES-modified mica. On this surface, the cations of the amine-terminated monolayer facilitate condensate formation instead of cations in solution. It is proposed that the APTES plays the role of the cations in inducing these structures to form by mediating interactions between the negatively charged DNA strands.[9] In this sense, the APTES monolayer serves as a useful model to the spermine/spermidine system, because the terminating amine group is similar to the basic functional groups of spermine and spermidine. In addition, as pointed out by Allen and co-workers,[7] eukaryotic DNA condensation on a surface may more closely approximate the native process because *in vivo* the movement of DNA is limited by a protein scaffold and the nuclear matrix. We note that prokaryotic DNA has not been observed to undergo

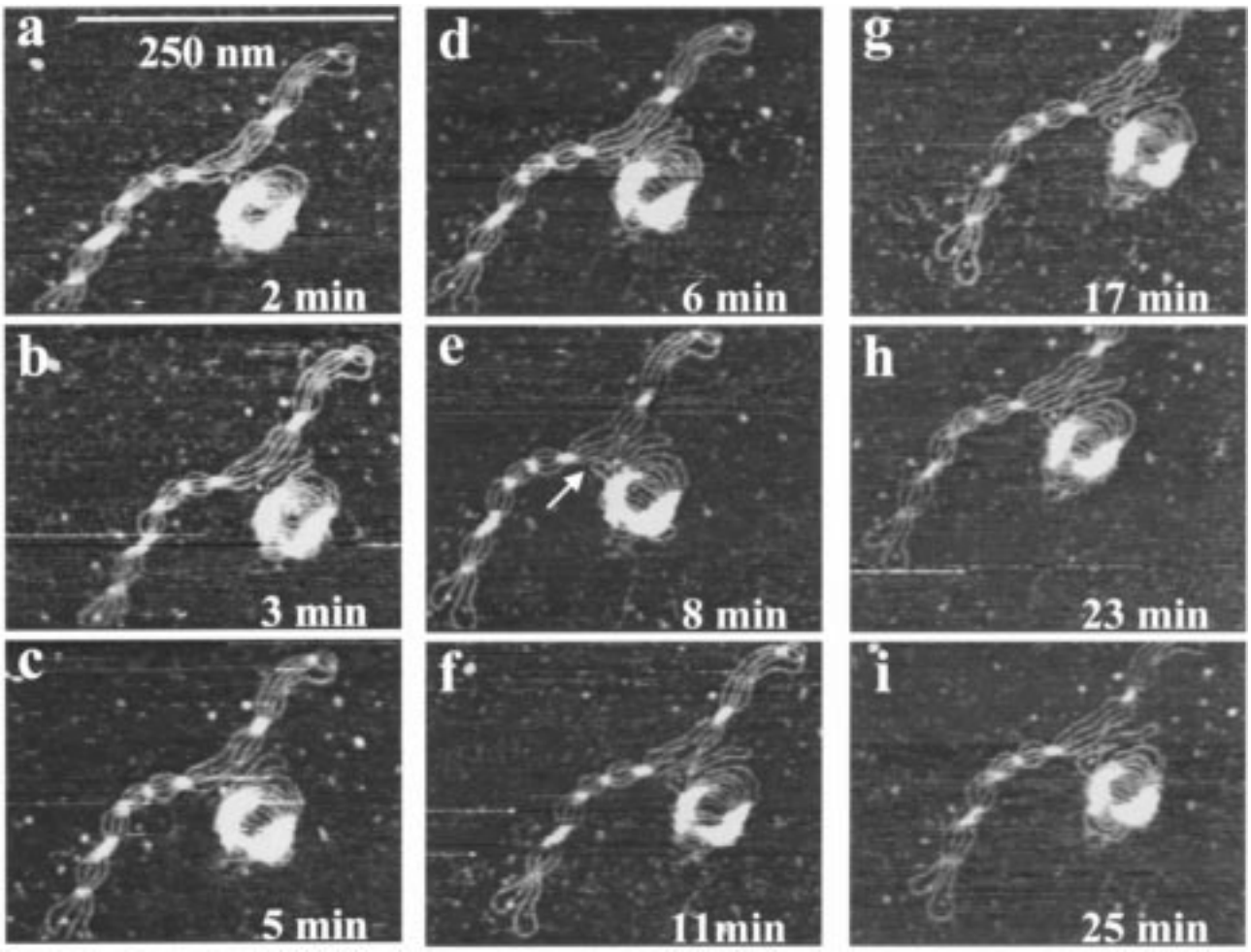

Figure 3. Time series of inter-condensate dynamics. Images collected at (a) 2, (b) 3, (c) 5, (d) 6, (e) 8, (f) 11, (g) 17, (h) 23, and (i) 25 min following Figure 2. The scale indicated in panel a applies to all images.

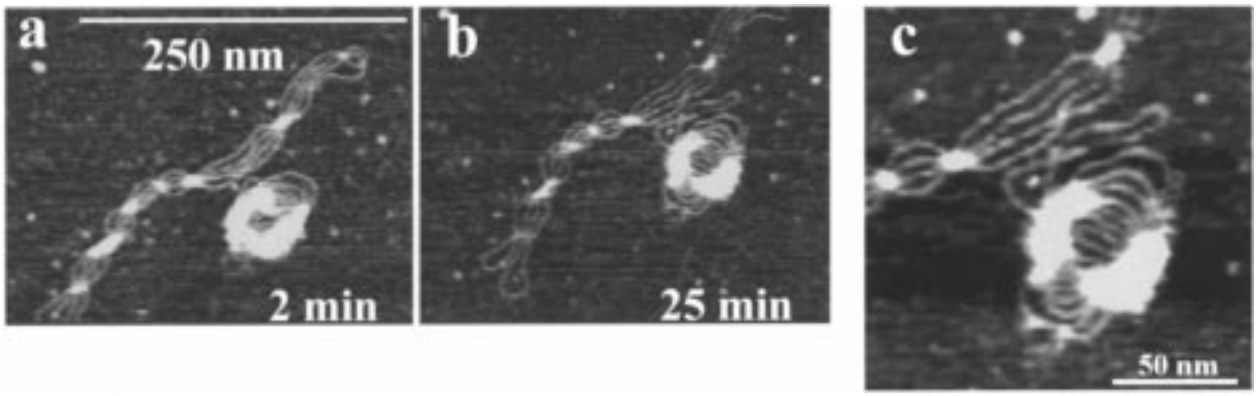

Figure 4. Summary of observed dynamics between linear and toroidal condensates: (a) 2 min image, (b) 25 min image, and (c) magnification of panel b. The scale in panel a applies to panel b.

condensation during cellular reproduction unlike eukaryotic DNA during mitosis or meiosis. It is possible that the condensation we observe is a model of the prokaryotic equivalent.

We can confirm that DNA attached to the surface of chemically modified mica is mobile. In the past, we have observed the movement of supercoiled DNA on a surface in an aqueous environment, as reported previously by Lyubchenko and Shlyakhtenko.[17] This indicates that the DNA is not bound so strongly as to make it immobile. Consequently, we can infer that the forces that drive condensation are stronger than those that bind DNA and DNA condensates to chemically modified mica, a conclusion drawn by Allen[7] and others. Interestingly, the motion of **B** has been much more than that of **A**. While the crossover point of **A** has moved somewhat during the experiment and the strands of **A** have moved considerably, **B** has been relatively mobile. This may be because **B** is largely 3-dimensional, at least initially, and fewer strands are in contact with the surface. The main point is that the motion of **B** is near and in response to **A**. Even in the first acquired image (Figure 2), we see indication of **B** motion where the **B** loop (near the arrow) is pointed directly toward the crossover point of **A**. Likewise, **A** responds to motion of **B**.

It is important to note that the salt concentration increases during the time series of Figure 3. As the aqueous drop on the

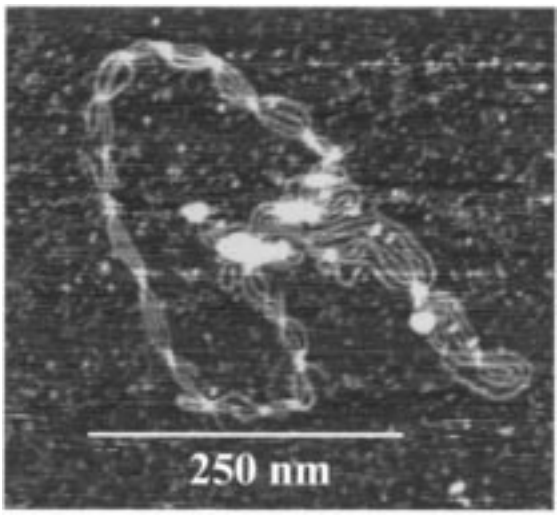

Figure 5. Multi-condensate intermediate structure formed from several linear structures.

surface evaporates during the experiment, the volume of water decreases. If we assume a linear decrease in volume with time and if 20% of the water volume remains at the end of the time series, then the salt concentration will have increased 5-fold. This increased salt concentration is not near physiological ionic strength. In addition, although buffer salt concentration increases, we do not expect the components of the buffer to be particularly efficient at DNA charge screening. Hence, we do not attribute these dynamics to an increase in a low concentration buffer.

It is clear from Figures 3 and 4 that a level of organization among the strands has occurred. The strands of both **A** and **B** have arranged themselves in a roughly equidistant and parallel fashion as shown in Figure 4c. It seems unlikely that such an organized structure would be formed from random motion of the component strands. Intermediates of parallel strands in condensate formation are found by Bloomfield,[1] Dunlap,[3] and Allen.[7] Formation of the crossover point of the pertinent strand of **B** at 8 min (Figure 3e) indicates quite a perturbation to the 4 proximal strands of **A**. In addition, by the end of the time series, the crossover points of **A** and **B** are in close proximity and the strands of **A** are parallel, approximately equidistant, and commensurate with those of **B**. This observation indicates that these crossover points or topological defects govern and drive multi-condensate formation. These findings are consistent with those of Dunlap and co-workers.[3]

Furthermore, our findings are in qualitative agreement with the electron microscopy study by Bottcher and co-workers. Bottcher *et al*.[6] imaged intermediates between linear and toroidal structures *via* cryoelectron microscopy. DNA condensation was induced by spermine and uranyl acetate. The extent of condensation was controlled by the concentration of uranyl salts. At lower salt concentrations, intermediate structures in the formation of condensates were imaged. They found connected linear structures of parallel DNA strands. These were followed at higher salt concentrations by cylindrical bundles. In turn, these bundles were followed at still higher salt concentration by toroids. They inferred that the toroids were formed from the coiled bundles and the coiled bundles were formed from the linear, parallel stranded structures.

From these EM images, Bottcher *et al*. proposed a mechanism for condensate formation. First, counterions screen DNA charge. In our work, the counterion is provided by APTES, as described by Fang and Hoh.[9] Then, parallel strands form followed by hydrophobicity minimization from the bound protein. Since we have not introduced an enzyme in our work, we do not expect to see much 3-dimensional structure. Still, we observe toriods and other condensate structures. Hydrophobicity may be supplied by the APTES monolayer. It has been suggested that individual aminopropyltriethoxysilane molecules are mobile at the surface.[9] In addition, these mobile species may be part of the crossover points that are areas of high contrast in the images. In any case, the inter-condensate intermediate that we observe is consistent with the early portion of this proposed mechanism for toroid formation.

On the basis of the results presented here, together with the aforementioned investigations, we propose that the observed inter-condensate structure is likely an early intermediate in multimeric condensate formation. It is plausible that a multimeric condensate structure is imminent because we have observed many images representative of that shown in Figure 5. The multi-condensate structure in Figure 5 may be interpreted as linear, roughly cylindrical structures about to coil into a toroid. Furthermore, we interpret the toroid of Figure 1c as a coiled-linear structure. This hypothesis is suggested by Dunlap *et al*.[3] as well.

Conclusions

Atomic force microscopy was used to investigate the dynamics of bacterial plasmid DNA condensates under aqueous buffer. The AFM images provided here represent the first direct evidence of condensate interaction at the solid−liquid interface in real-time. This interaction results in self-assembly of the component DNA strands. We suggest that this intermediate is a precursor to a larger condensate. This hypothesis is consistent with those proposed from previous studies of intermediate structures observed *ex situ* by EM and AFM and *in situ* by AFM (Dunlap *et al*.). Many questions remain regarding the dynamics of DNA and DNA condensates at the solid−liquid interface. Given that these questions bear on understanding DNA compaction in cellular processes, AFM studies will continue and may help to clarify these mechanisms. Toward this end, we are currently working on an experimental design that will allow us to image for longer periods of time while maintaining high resolution.

Acknowledgment. The authors gratefully acknowledge the National Science Foundation (Leveraged Starter Grant, Research Planning Grant, and Presidential Early Career Award for Scientists and Engineers), Dreyfus Foundation, Research Corporation, ACS-PRF, Occidental College, and the Howard Hughes Medical Institute for generous financial support. E.M.S. is grateful to Professor Mark O. Martin, Department of Biology, Occidental College, for his expertise. We thank Professors Jens P. Franck and Grace Fisher-Adams, Department of Biology, Occidental College, for helpful information. Finally, we thank Ms. Mui Sam and Ms. Karen Stella for laboratory assistance and Mr. Kenneth Woodruff for computing assistance.

JA9915697